Dyakonov-Tamm waves guided by the interface between two structurally chiral materials that differ only in handedness

Jun Gao,[1,2] Akhlesh Lakhtakia,[1,*] and Mingkai Lei[2]

[1]*NanoMM–Nanoengineered Metamaterials Group, Department of Engineering Science and Mechanics, Pennsylvania State University, University Park, Pennsylvania 16802, USA*

[2]*Surface Engineering Laboratory, School of Materials Science and Engineering, Dalian University of Technology, Dalian 116024, People's Republic of China*

(Received 30 September 2009; published 4 January 2010)

The boundary-value problem of the propagation of Dyakonov-Tamm waves guided by the planar interface between two structurally chiral materials that are identical except for structural handedness was formulated and numerically solved. Detailed analysis showed that either two or three different Dyakonov-Tamm waves can propagate. These waves have different phase speeds and degrees of localization to the interface with a sudden handedness change. The most localized Dyakonov-Tamm waves are essentially confined to within a small number of structural periods of the interface on either side.

DOI: 10.1103/PhysRevA.81.013801 PACS number(s): 42.25.−p, 42.70.−a

I. INTRODUCTION

A structurally chiral material (SCM), such as a chiral liquid crystal [1,2] or a chiral sculptured thin film (STF) [3,4], has a periodic nonhomogeneity which is born of a continuous rotation of anisotropic dielectric properties at a uniform rate along a specific axis. Structurally, an SCM can be either left-handed or right-handed. When illuminated by circular polarized light, an SCM exhibits the circular Bragg phenomenon as follows. Provided the SCM is sufficiently thick and the free-space wavelength of incident light lies in a regime called the Bragg regime that depends on the angle of incidence with respect to the axis of chirality, over a wide range of angles of incidence the reflectance is either very high or very low—depending on whether the illuminating light and the SCM are co-handed or cross-handed [5–7]. Thus, an SCM acts as a circular-polarization filter, a characteristic that is best appreciated when the wave vector of the illuminating light is parallel to the axis of chirality.

The polarization dependence vanishes if two SCMs, identical in all respects but differing in structural handedness, are stacked on top of each other, provided that dissipation in the SCM is sufficiently weak [8–10]. Thus, the differing structural handednesses can offset the differing circular-polarization sensitivities of the two SCMs in this arrangement. The question of whether the planar interface of two such SCMs can guide the propagation of surface waves arose. If so, these surface waves are to be classified as Dyakonov-Tamm waves [11–13], which combine the features of Dyakonov surface waves [14–22] and Tamm states [23–27] and arose from research [11] on surface-wave propagation guided by the planar interface of a chiral STF and an isotropic dielectric material. These waves were also shown to be allowed by a twist-defect interface in an SCM [13,28].

Dyakonov surface waves propagate at the planar interface of two homogeneous, nonconducting, dielectric materials, at least one of which is anisotropic. As these surface waves can exist only when very restrictive conditions are satisfied [29,30], their existence was experimentally confirmed [31] some two decades after the theoretical prediction of their existence [14]. Dyakonov surface waves have several potential applications in integrated optics [32–34]. Electronic states called Tamm states are localized to the surface of a solid occupying a half space. These states were experimentally observed in 1990 on the surfaces of superlattices [24], and their optical analogs have been theoretically investigated subsequently [25–27].

Our aim here is to establish the possibility of the propagation of Dyakonov-Tamm waves guided by the planar interface of two SCMs that are identical except for structural handedness. For generality, we also assume that either of the SCMs is twisted arbitrarily with respect to the direction of propagation of the Dyakonov-Tamm wave parallel to the interface. Section II presents the relevant boundary-value problem which yields the dispersion equation for Dyakonov-Tamm waves. Section III contains numerical results and discussions for an SCM that is a chiral STF made of titanium oxide. An $\exp(-i\omega t)$ time dependence is implicit, with ω denoting the angular frequency. The free-space wave number, the free-space wavelength, and the intrinsic impedance of free space are denoted by $k_0 = \omega\sqrt{\varepsilon_0\mu_0}$, $\lambda_0 = 2\pi/k_0$, and $\eta_0 = \sqrt{\mu_0/\varepsilon_0}$, respectively, with μ_0 and ε_0 being the permeability and permittivity of free space, respectively. Vectors are underlined once, dyadics are underlined twice, column vectors are underlined and enclosed within square brackets, and matrices are underlined twice and similarly bracketed. Cartesian unit vectors are identified as u_x, u_y, and u_z. The dyadics employed in the following sections can be treated as 3×3 matrices [35,36].

II. FORMULATION

A. Geometry and permittivity dyadics

Let the half-space $z > 0$ be occupied by an SCM with a unidirectionally nonhomogeneous, frequency-dependent permittivity dyadic given by [3,4]

$$\underline{\underline{\varepsilon}}(z) = \varepsilon_0 \underline{\underline{S}}_z(z, h, \Omega, \gamma^+) \cdot \underline{\underline{S}}_y(\chi) \cdot \underline{\underline{\varepsilon}}_{\text{ref}} \cdot \underline{\underline{S}}_y^T(\chi) \cdot \underline{\underline{S}}_z^T(z, h, \Omega, \gamma^+), \quad z > 0 \tag{1}$$

*akhlesh@psu.edu

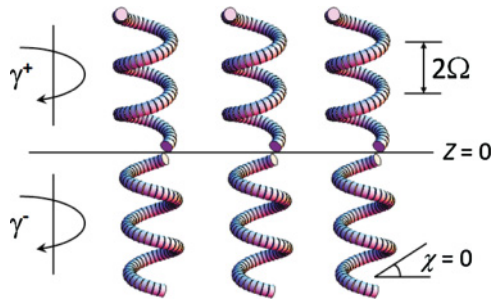

FIG. 1. (Color online) Schematic of the planar interface of two chiral STFs that are identical except for their different structural-handedness parameters.

and the half-space $z < 0$ by an SCM characterized by

$$\underline{\underline{\varepsilon}}(z) = \varepsilon_0 \underline{\underline{S}}_z(z, -h, \Omega, \gamma^-) \cdot \underline{\underline{S}}_y(\chi) \cdot \underline{\underline{\varepsilon}}_{\text{ref}} \cdot \underline{\underline{S}}_y^T(\chi) \cdot \underline{\underline{S}}_z^T(z, -h, \Omega, \gamma^-), \quad z < 0, \tag{2}$$

where the reference relative permittivity dyadic,

$$\underline{\underline{\varepsilon}}_{\text{ref}} = \varepsilon_a \underline{u}_z \underline{u}_z + \varepsilon_b \underline{u}_x \underline{u}_x + \varepsilon_c \underline{u}_y \underline{u}_y, \tag{3}$$

indicates local orthorhombic symmetry. The dyadic function

$$\underline{\underline{S}}_z(z, \pm h, \Omega, \gamma^\pm) = (\underline{u}_x \underline{u}_x + \underline{u}_y \underline{u}_y) \cos\zeta_\pm \pm h(\underline{u}_y \underline{u}_x - \underline{u}_x \underline{u}_y) \sin\zeta_\pm + \underline{u}_z \underline{u}_z, \tag{4}$$

where

$$\zeta_\pm = \frac{\pi z}{\Omega} + \gamma^\pm, \tag{5}$$

contains 2Ω as the structural period and $\pm h$ as the structural-handedness parameters. The parameter $h = 1$ ($h = -1$) indicates right (left)-handedness for the SCM in half-space $z > 0$ and left (right)-handedness for the SCM in half-space $z < 0$.

The beginning of the helical variation of the permittivity dyadic is offset relative to the x axis in the x-y plane by an angle $\gamma^+ \in [-\pi, \pi]$ in the half-space $z > 0$ and by an angle $\gamma^- \in [-\pi, \pi]$ in the half-space $z < 0$. The tilt dyadic

$$\underline{\underline{S}}_y(\chi) = (\underline{u}_x \underline{u}_x + \underline{u}_z \underline{u}_z) \cos\chi + (\underline{u}_z \underline{u}_x - \underline{u}_x \underline{u}_z) \sin\chi + \underline{u}_y \underline{u}_y \tag{6}$$

involves the angle of inclination χ with respect to the x-y plane. The superscript T denotes the transpose. The relative permittivity scalars ε_a, ε_b, and ε_c are functions of the angular frequency. Equations (1)–(6) can represent chiral nematic and chiral smectic liquid crystals, as well as chiral STFs.

B. Field representation

Keeping both angles γ^+ and γ^- arbitrary, we take the Dyakonov-Tamm wave to propagate parallel to the x axis in the x-y plane. Then the fields are independent of the y coordinate, and it is appropriate to write [3]

$$\left.\begin{aligned} \underline{E}(\underline{r}) &= \underline{e}(z) \exp(i\kappa x) \\ \underline{H}(\underline{r}) &= \underline{h}(z) \exp(i\kappa x) \end{aligned}\right\} \forall\, z. \tag{7}$$

The column vector

$$[\underline{f}(z)] = [\,\underline{e}_x(z)\ \underline{e}_y(z)\ \underline{h}_x(z)\ \underline{h}_y(z)\,]^T \tag{8}$$

satisfies the matrix differential equation [6],

$$\frac{d}{dz}[\underline{f}(z)] = i[\underline{\underline{P}}^\pm(z, \kappa)] \cdot [\underline{f}(z)] \left.\begin{matrix} \\ \end{matrix}\right\} \begin{matrix} z > 0 \\ z < 0 \end{matrix}, \tag{9}$$

where the 4×4 matrix

$$[\underline{\underline{P}}^\pm(z, \kappa)] = \omega \begin{bmatrix} 0 & 0 & 0 & \mu_0 \\ 0 & 0 & -\mu_0 & 0 \\ \pm h\varepsilon_0(\varepsilon_c - \varepsilon_d)\cos\zeta_\pm \sin\zeta_\pm & -\varepsilon_0(\varepsilon_c \cos^2\zeta_\pm + \varepsilon_d \sin^2\zeta_\pm) & 0 & 0 \\ \varepsilon_0(\varepsilon_c \sin^2\zeta_\pm + \varepsilon_d \cos^2\zeta_\pm) & \mp h\varepsilon_0(\varepsilon_c - \varepsilon_d)\cos\zeta_\pm \sin\zeta_\pm & 0 & 0 \end{bmatrix} + \kappa \frac{\varepsilon_d(\varepsilon_a - \varepsilon_b)}{\varepsilon_a \varepsilon_b} \sin\chi \cos\chi \begin{bmatrix} \cos\zeta_\pm & \pm h \sin\zeta_\pm & 0 & 0 \\ 0 & 0 & 0 & 0 \\ 0 & 0 & 0 & \mp h \sin\zeta_\pm \\ 0 & 0 & 0 & \cos\zeta_\pm \end{bmatrix} + \begin{bmatrix} 0 & 0 & 0 & -\frac{\kappa^2}{\omega\varepsilon_0} \frac{\varepsilon_d}{\varepsilon_a \varepsilon_b} \\ 0 & 0 & 0 & 0 \\ 0 & \frac{\kappa^2}{\omega\mu_0} & 0 & 0 \\ 0 & 0 & 0 & 0 \end{bmatrix} \tag{10}$$

and

$$\varepsilon_d = \frac{\varepsilon_a \varepsilon_b}{\varepsilon_a \cos^2\chi + \varepsilon_b \sin^2\chi}. \tag{11}$$

Equation (9) can be solved by two independent techniques [37–39]. The ultimate aim is to determine the matrices $[\underline{\underline{N}}^\pm]$ that appear in the relations

$$[\underline{f}(\pm 2\Omega)] = [\underline{\underline{N}}^\pm] \cdot [\underline{f}(0\pm)] \tag{12}$$

to characterize the optical response of one period each of both SCMs. The matrices $[\underline{\underline{N}}^\pm]$ can be calculated using two numerical techniques: the piecewise uniform approximation technique [6] and a series technique based on the Maclaurin expansion of $[\underline{\underline{P}}^\pm(z, \kappa)]$ with respect to z [37,38]. As both

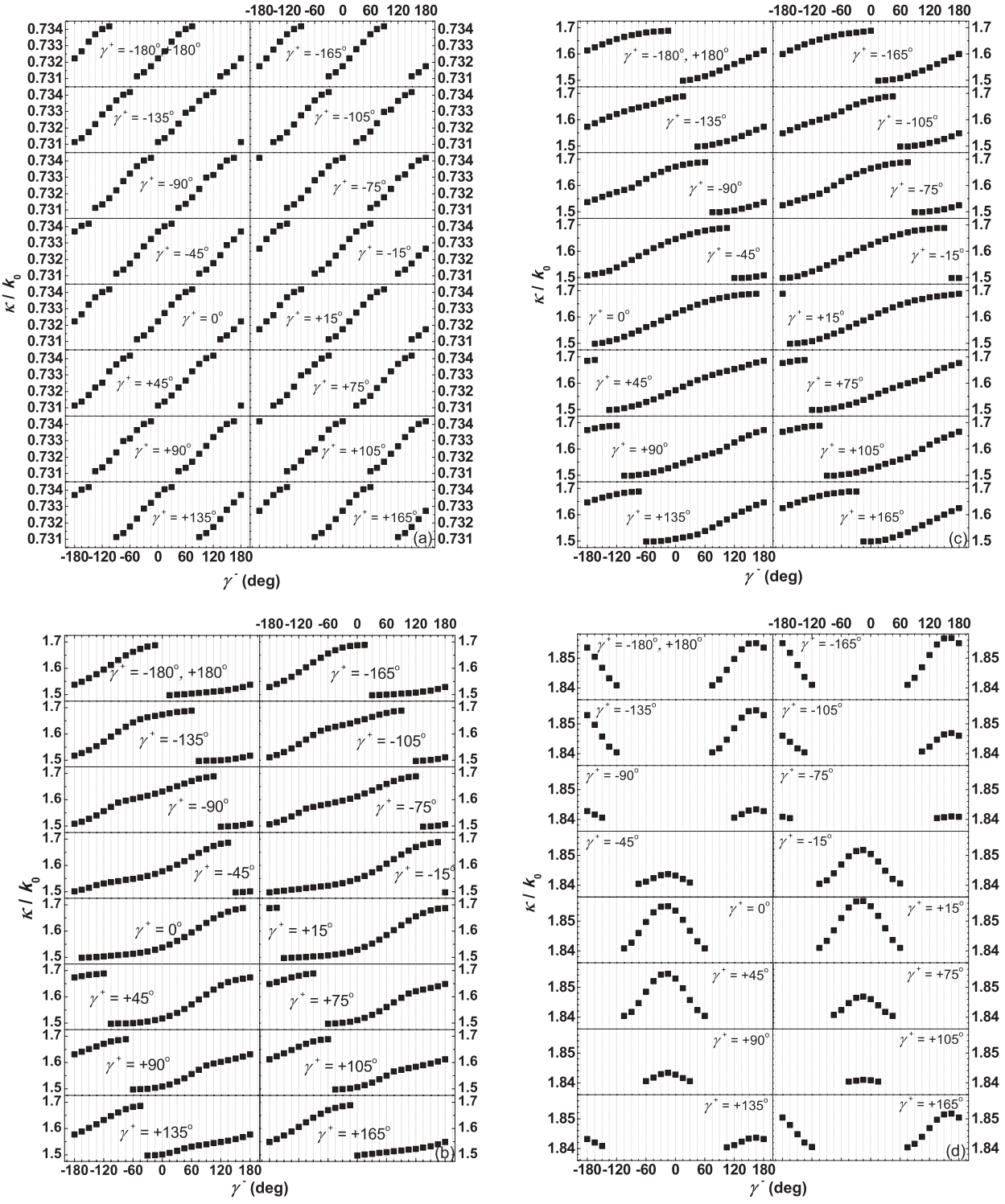

FIG. 2. Sets of solutions κ/k_0 of Eq. (20) for different combinations of the angular offsets γ^+ and γ^-: $\varepsilon_a = 2.514$, $\varepsilon_b = 3.943$, $\varepsilon_c = 3.153$, $\chi = 46.367^\circ$, $\Omega = 197$ nm, and $\lambda_0 = 633$ nm. (a) First set, (b) second set, (c) third set, and (d) fourth set.

techniques yield the same results [39], the piecewise uniform approximation technique was selected for all results reported here.

Basically, this technique consists of subdividing each period of the SCM into a cascade of electrically thin sublayers parallel to the plane $z = 0$ and assuming the dielectric properties to be spatially uniform in each sublayer. A sufficiently large number $N + 1$ points $z_n^{\pm} = \pm 2\Omega(n/N)$, $n \in [0, N]$, are defined on each side of the interface and the matrices

$$[\underline{\underline{W}}_n^{\pm}] = \exp\left\{\pm i\left[\underline{\underline{P}}^{\pm}\left(\frac{z_{n-1}^{\pm} + z_n^{\pm}}{2}, \kappa\right)\right]\frac{2\Omega}{N}\right\}, \quad n \in [1, N] \tag{13}$$

are calculated for a specific value of κ; then

$$[\underline{\underline{N}}^{\pm}] \cong [\underline{\underline{W}}_N^{\pm}] \cdot [\underline{\underline{W}}_{N-1}^{\pm}] \cdot \ldots \cdot [\underline{\underline{W}}_2^{\pm}] \cdot [\underline{\underline{W}}_1^{\pm}]. \quad (14)$$

A sublayer thickness $2\Omega/N = 2$nm gave reasonable results.

By virtue of the Floquet-Lyapunov theorem [40], we can define the matrices $[\underline{\underline{Q}}^{\pm}]$ such that

$$[\underline{\underline{N}}^{\pm}] = \exp\{\pm i 2\Omega [\underline{\underline{Q}}^{\pm}]\}. \quad (15)$$

Both $[\underline{\underline{N}}^{\pm}]$ and $[\underline{\underline{Q}}^{\pm}]$ share the same eigenvectors, and their eigenvalues are also related as follows. Let $[\underline{t}^{\pm}]^{(n)}$, $n \in [1, 4]$, be the eigenvector corresponding to the nth eigenvalue $\sigma_n^{\pm}$ of $[\underline{\underline{N}}^{\pm}]$; then, the corresponding eigenvalue $\alpha_n^{\pm}$ of $[\underline{\underline{Q}}^{\pm}]$ is given by

$$\alpha_n^{\pm} = \mp i \frac{\ln \sigma_n^{\pm}}{2\Omega}. \quad (16)$$

C. Dispersion equation for Dyakonov-Tamm wave

The electromagnetic fields of the Dyakonov-Tamm wave must diminish in magnitude as $z \to \pm\infty$; the faster the decay, the higher is the degree of localization to the interface. Therefore, in the half-space $z > 0$, we label the eigenvalues of $[\underline{\underline{N}}^{+}]$ such that $\mathrm{Im}[\alpha_{1,2}^{+}] > 0$ and then set

$$[\underline{f}(0+)] = [\,[\underline{t}^{+}]^{(1)}\ [\underline{t}^{+}]^{(2)}\,] \cdot \begin{bmatrix} A_1 \\ A_2 \end{bmatrix}, \quad (17)$$

where A_1 and A_2 are unknown scalars; the other two eigenvalues of $[\underline{\underline{N}}^{+}]$ describe fields that amplify as $z \to +\infty$ and cannot therefore contribute to the Dyakonov-Tamm wave. A similar argument for the half-space $z < 0$ requires us to ensure that $\mathrm{Im}[\alpha_{1,2}^{-}] < 0$ and then set

$$[\underline{f}(0-)] = [\,[\underline{t}^{-}]^{(1)}\ [\underline{t}^{-}]^{(2)}\,] \cdot \begin{bmatrix} B_1 \\ B_2 \end{bmatrix}, \quad (18)$$

where B_1 and B_2 are unknown scalars.

Continuity of the tangential components of the electric and magnetic fields across the interface $z = 0$ requires that $[\underline{f}(0+)] = [\underline{f}(0-)]$, which may be rearranged as

$$[\underline{\underline{M}}] \cdot \begin{bmatrix} A_1 \\ A_2 \\ B_1 \\ B_2 \end{bmatrix} = \begin{bmatrix} 0 \\ 0 \\ 0 \\ 0 \end{bmatrix}. \quad (19)$$

For a nontrivial solution, the 4×4 matrix $[\underline{\underline{M}}]$ must be singular, so that

$$\det[\underline{\underline{M}}] = 0 \quad (20)$$

is the dispersion equation for the Dyakonov-Tamm wave.

III. NUMERICAL RESULTS AND DISCUSSION

A. Preliminaries

In order to illustrate the results of solving Eq. (20), we decided to use chiral STFs as SCMs, as shown in Fig. 1. For definiteness, we set $h = 1$. The angles $\gamma^{+} \in [-\pi, \pi]$ and $\gamma^{-} \in [-\pi, \pi]$ were left as variable parameters. All calculations were carried out at $\lambda_0 = 633$nm with data previously used for chiral STFs made of titanium oxide [11]: $\varepsilon_a = 2.514$, $\varepsilon_b = 3.943$, $\varepsilon_c = 3.153$, $\chi = 46.367^{\circ}$, and $\Omega = 197$ nm.

A sequential combination of standard numerical methods—the search, the bisection, and the Newton-Raphson methods [41]—was employed to find values of κ that satisfy Eq. (20). If a solution exists, then ω/κ is the corresponding phase speed.

For every value of κ that satisfies Eq. (20), the fields on either side of the interface $z = 0$ were calculated as follows. First, we set $A_1 = 1$ V/m and calculated A_2, B_1, and B_2 from Eq. (19); then we obtained $[\underline{f}(0\pm)]$ from Eqs. (17) and (18); and finally we used

$$\begin{bmatrix} e_x(z_n^{\pm}) \\ e_y(z_n^{\pm}) \\ h_x(z_n^{\pm}) \\ h_y(z_n^{\pm}) \end{bmatrix} \cong [\underline{\underline{W}}_n^{\pm}] \cdot [\underline{\underline{W}}_{n-1}^{\pm}] \cdot \ldots \cdot [\underline{\underline{W}}_2^{\pm}] \cdot [\underline{\underline{W}}_1^{\pm}] \cdot [\underline{f}(0\pm)], \quad n \in [1, \infty], \quad (21)$$

$$h_z(z_n^{\pm}) = \left(\frac{\kappa}{\omega\mu_0}\right) e_y(z_n^{\pm}), n \in [1, \infty], \quad (22)$$

$$e_z(z_n^{\pm}) = \left(\frac{\varepsilon_d}{\varepsilon_a \varepsilon_b}\right) \left\{ -\left(\frac{\kappa}{\omega\varepsilon_0}\right) h_y(z_n^{\pm}) + (\varepsilon_a - \varepsilon_b) \frac{\sin 2\chi}{2} \left[e_x(z_n^{\pm}) \cos\left(\frac{\pi}{\Omega} z_n^{\pm} + \gamma^{\pm}\right) \pm h e_y(z_n^{\pm}) \sin\left(\frac{\pi}{\Omega} z_n^{\pm} + \gamma^{\pm}\right) \right] \right\}, \quad n \in [1, \infty). \quad (23)$$

B. Solutions of the dispersion equation

For each combination of γ^{+} and γ^{-}, we obtained up to four solutions of Eq. (20) that indicate the *possible* propagation of a Dyakonov-Tamm wave. The variations of computed values of κ/k_0 with γ^{-} at every chosen γ^{+} for all four sets of solutions are shown in Fig. 2. Because $\gamma^{\pm} = \pi$ is physically the same as $\gamma^{\pm} = -\pi$, the solution at $\gamma^{-} = \pi$ is equal to the one at $\gamma^{-} = -\pi$ for any $\gamma^{+} \in [-\pi, \pi]$, and vice versa.

The first set of solutions, shown in Fig. 2(a), has values of the relative wavenumber κ/k_0 around 0.734. This set is organized in two parallel branches separated by two 60° gaps on the γ^{-} axis in which no solution exists; κ/k_0 increases with the increase of γ^{-} in each branch. The values of γ^{-} at

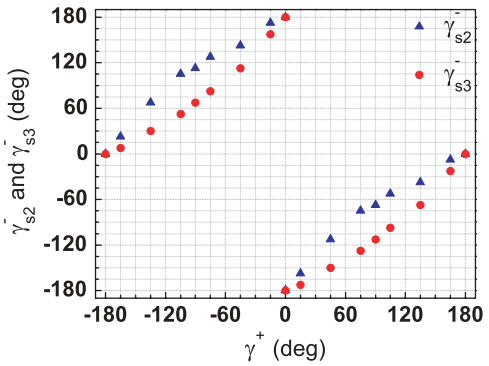

FIG. 3. (Color online) γ_{s2}^{-} and γ_{s3}^{-} as functions of γ^{+}.

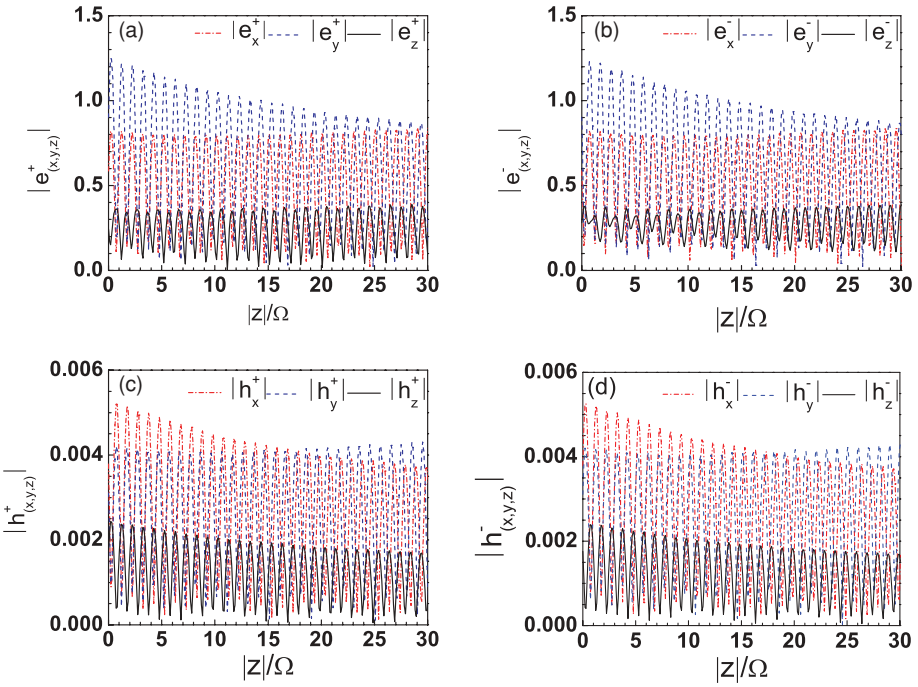

FIG. 4. (Color online) Profiles of the magnitudes of field components of the first solution ($\kappa/k_0 = 0.734025$) of Eq. (20) for $\gamma^+ = 15^\circ$ and $\gamma^- = -105^\circ$. Electric field magnitudes are in V/m, and magnetic field magnitudes are in A/m, with $A_1 = 1$ V/m. Field components in the half-space $z > 0$ are superscripted $+$, whereas those in the half-space $z < 0$ are superscripted $-$. See Fig. 2 for the values of the constitutive and geometric parameters used.

the midpoints of the two gaps are given by

$$\gamma_{s11}^- = \begin{cases} \gamma^+ + \frac{7}{12}\pi, & \gamma^+ \in [-\pi, \frac{5}{12}\pi] \\ \gamma^+ + \frac{7}{12}\pi - 2\pi, & \gamma^+ \in [\frac{5}{12}\pi, \pi] \end{cases} \quad (24)$$

and

$$\gamma_{s12}^- = \begin{cases} \gamma^+ + \frac{19}{12}\pi, & \gamma^+ \in [-\pi, -\frac{7}{12}\pi] \\ \gamma^+ + \frac{19}{12}\pi - 2\pi, & \gamma^+ \in [-\frac{7}{12}\pi, \pi]. \end{cases} \quad (25)$$

The variations of κ/k_0 in the second and the third sets of solutions with γ^- for specific values of γ^+ are shown in Figs. 2(b) and 2(c), respectively. For each set, the solutions lie on a single curve which contains a discontinuity at a value of γ^- denoted by γ_{s2}^- and γ_{s3}^- for the two sets. Both γ_{s2}^- and γ_{s3}^- are plotted against γ^+ in Fig. 3, which shows that they are farthest apart in the neighborhood of $\gamma^+ = \pm\pi/2$.

The fourth set of solutions, with κ/k_0 around 1.84, is shown in Fig. 2(d). Solutions in this set do not exist for all combinations of γ^+ and γ^-. If the γ^- axis is folded so that $\gamma^- = -\pi$ and $\gamma^- = \pi$ are joined, the solutions for a specific value of γ^+ lie on a symmetric curve with one maximum.

Although all four sets are solutions of Eq. (20), they do not necessarily indicate the propagation of surface waves. Therefore, the variations of the electric and magnetic fields with z were examined for several representative solutions from

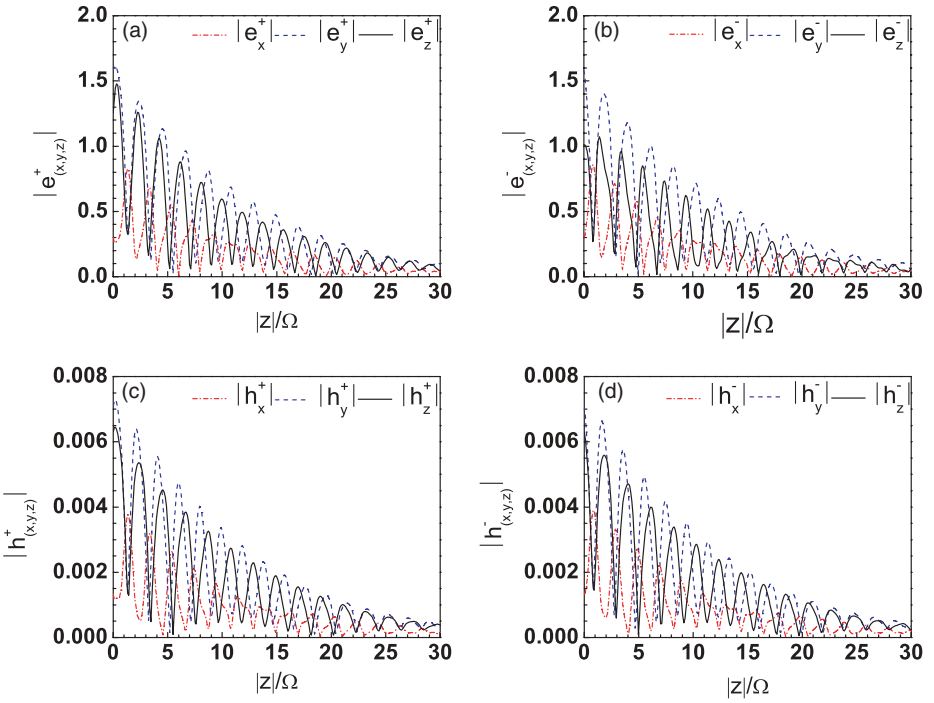

FIG. 5. (Color online) Same as Fig. 4, but for the second solution ($\kappa/k_0 = 1.501607$) of Eq. (20) for $\gamma^+ = 15^\circ$ and $\gamma^- = -105^\circ$.

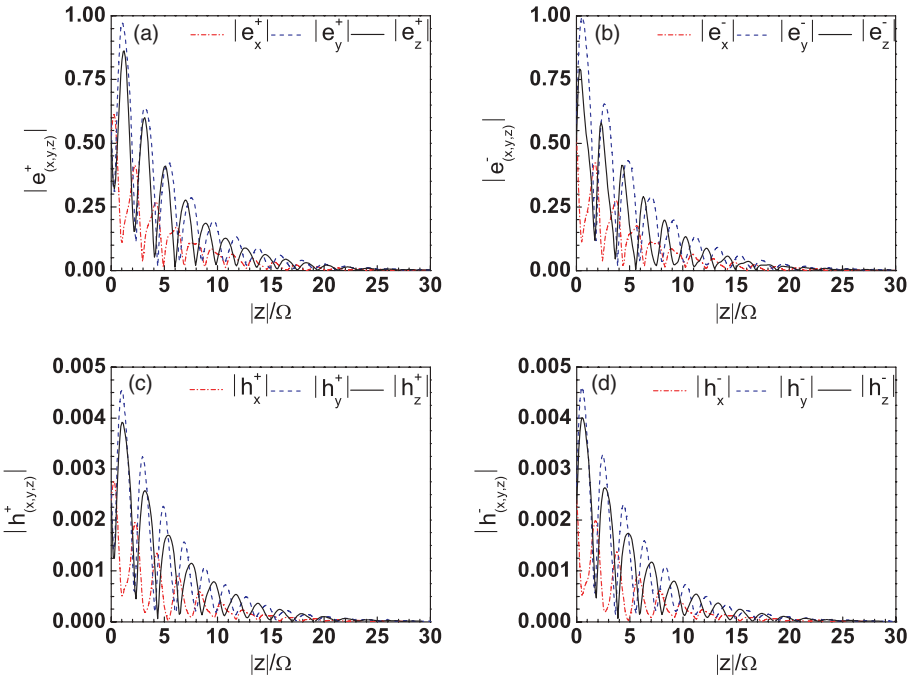

FIG. 6. (Color online) Same as Fig. 4, but for the third solution ($\kappa/k_0 = 1.516921$) of Eq. (20) for $\gamma^+ = 15^\circ$ and $\gamma^- = -105^\circ$.

the four sets. The field profiles on the two sides of the interface $z = 0$ are, in general, different from each other. The profiles for $\gamma^+ = 15^\circ$ and $\gamma^- = -105^\circ$ were chosen for presentation here since all four solutions of Eq. (20) exist for this combination of the two angular offsets. We see that the fields for the first solution ($\kappa/k_0 = 0.734025$) in Fig. 4 are not localized at all to the interface $z = 0$, indicating they do not belong to a surface wave. The field profiles for the second ($\kappa/k_0 = 1.501607$) and the third ($\kappa/k_0 = 1.516921$) solutions are presented in Figs. 5 and 6, respectively. Both solutions have different field profiles, but both are strongly coupled to the interface. Finally, the fields for the fourth solution ($\kappa/k_0 = 1.840987$) presented in Fig. 7 are superpositions of a strongly localized component and a weakly localized component. These field profiles allow us to conclude that three different Dyakonov-Tamm waves can propagate for the chosen combination of γ^+ and γ^-. The most localized Dyakonov-Tamm waves are essentially confined to within three structural periods on either side of the interface; that is, their fields are concentrated in the zone $|z| < 6\Omega$.

The degree of localization to the interface is described by four decay constants: $\exp(-u_1)$, $\exp(-u_2)$, $\exp(-v_1)$, and $\exp(-v_2)$, where $u_{1,2} = \mathrm{Im}[\alpha^+_{1,2}] \cdot 2\Omega$ and $v_{1,2} = -\mathrm{Im}[\alpha^-_{1,2}] \cdot 2\Omega$. As the constraints $\mathrm{Im}[\alpha^+_{1,2}] > 0$ and $\mathrm{Im}[\alpha^-_{1,2}] < 0$ must be satisfied for a Dyakonov-Tamm wave to exist, all decay constants should be less than unity for the wave to decay as $z \to \pm\infty$. The smaller that the decay constants are, the

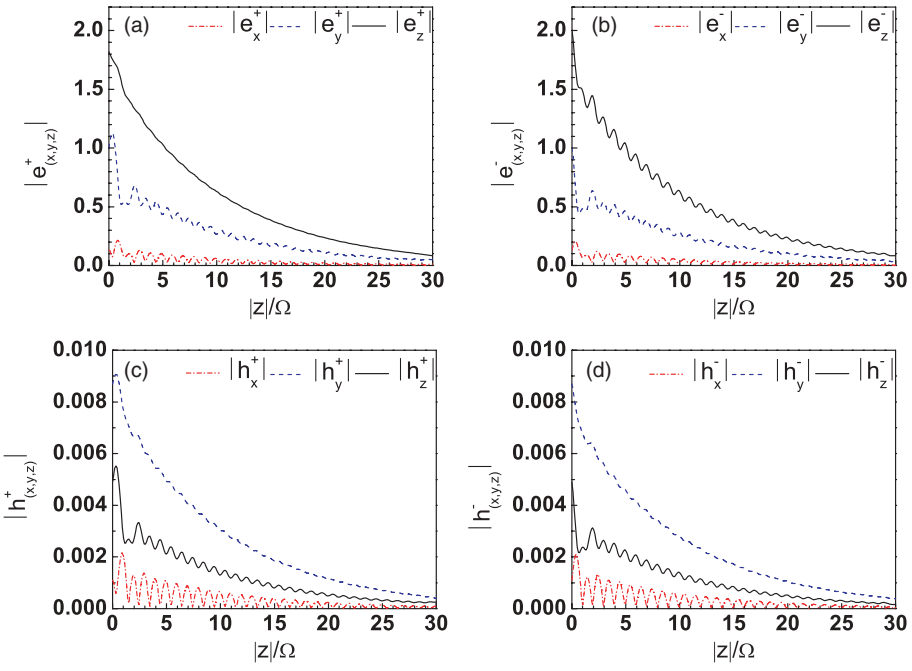

FIG. 7. (Color online) Same as Fig. 4, but for the fourth solution ($\kappa/k_0 = 1.840987$) of Eq. (20) for $\gamma^+ = 15^\circ$ and $\gamma^- = -105^\circ$.

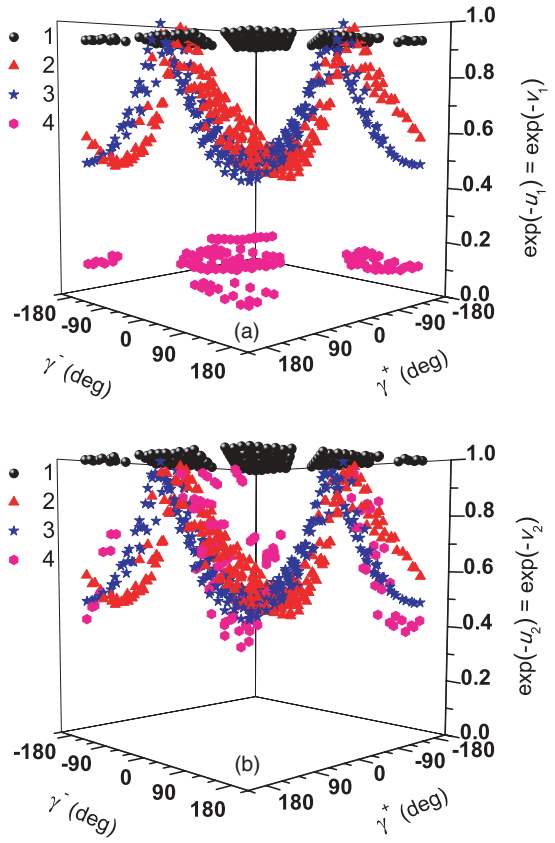

FIG. 8. (Color online) Variations of decay constants $\exp(-u_1) = \exp(-v_1)$ and $\exp(-u_2) = \exp(-v_2)$ with the angular offsets $\gamma^{\pm}$. See Fig. 2 for the values of the constitutive and geometric parameters used.

stronger is the wave localized to the interface. We therefore examined the decay constants as functions of the angular offsets. The eigenvalues, but not the eigenvectors, of $[\underline{\underline{N}}^{\pm}]$ are independent of $\gamma^{\pm}$. Furthermore, as $\alpha^{+}_{1,2} = -\alpha^{-}_{1,2}$, $\exp(-u_1) = \exp(-v_1)$ and $\exp(-u_2) = \exp(-v_2)$, so that at most two decay constants are possible. For the second and third sets of solutions, $\alpha^{+}_{1} = \alpha^{+}_{2}$ and $\alpha^{-}_{1} = \alpha^{-}_{2}$, so there is only one decay constant $\exp(-u_1) = \exp(-v_1) = \exp(-u_2) = \exp(-v_2)$.

The decay constants are plotted in Fig. 8 as functions of γ^{+} and γ^{-}. For the first set of solutions, we see that $\exp(-u_1) = \exp(-v_1) < 1$ and $\exp(-u_2) = \exp(-v_2) \approx 0.999\ldots$. Clearly, then $u_2 = v_2$ is almost null valued, which means that the relevant solutions of Eq. (20) do not signify the propagation of Dyakonov-Tamm waves, confirming our suspicion from Fig. 4. For the second and the third sets of solutions, we obtain $\exp(-u_1) = \exp(-v_1) = \exp(-u_2) = \exp(-v_2) < 1$. The sole decay constant for the second set of solutions represented by red triangles in Fig. 8 has the smallest value at $\{\gamma^{+} = -135^{\circ}, \gamma^{-} = -90^{\circ}\}$, $\{\gamma^{+} = -90^{\circ}, \gamma^{-} = -45^{\circ}\}$, $\{\gamma^{+} = 45^{\circ}, \gamma^{-} = 90^{\circ}\}$, and $\{\gamma^{+} = 90^{\circ}, \gamma^{-} = 135^{\circ}\}$, thereby indicating the strongest localization. The sole decay constant for the third set represented by blue stars in the same figure has the smallest value at $\{\gamma^{+} = -105^{\circ}, \gamma^{-} = -90^{\circ}\}$, $\{\gamma^{+} = -90^{\circ}, \gamma^{-} = -75^{\circ}\}$, $\{\gamma^{+} = 75^{\circ}, \gamma^{-} = 90^{\circ}\}$, and $\{\gamma^{+} = 90^{\circ}, \gamma^{-} = 105^{\circ}\}$. The two decay constants in Fig. 8 for the fourth set of the solutions also signify the propagation of Dyakonov-Tamm waves for certain combinations of γ^{+} and γ^{-}, because $\exp(-u_1) = \exp(-v_1) < 1$ and $\exp(-u_2) = \exp(-v_2) < 1$, but with one strongly localized component and one weakly localized component.

We conclude from the foregoing figures that Dyakonov-Tamm waves can propagate guided by the interface $z = 0$, whether any angular offsets are present or not.

IV. CONCLUDING REMARKS

We formulated the boundary-value problem of the propagation of Dyakonov-Tamm waves guided by the planar interface of two SCMs that are identical except for structural handedness. The angular offsets $\gamma^{\pm}$ of beginning the helical variation relative to the x axis in the x-y plane were varied arbitrarily. A material discontinuity across the interface exists even when both offsets are null valued. By numerically solving a dispersion equation, we found that, depending on the angular offsets, either two or three different Dyakonov-Tamm waves can propagate—with different phase speeds and degrees of localization to the interface. The most localized Dyakonov-Tamm waves are essentially confined to within three structural periods of the interface on either side.

ACKNOWLEDGMENTS

JG gratefully acknowledges the financial support of the Chinese Scholarship Council (CSC). AL thanks the Charles Godfrey Binder Endowment at Penn State for ongoing support of his research activities.

[1] P. G. de Gennes and J. Prost, *The Physics of Liquid Crystals* (Clarendon Press, Oxford, United Kingdom, 1993).
[2] W. E. Haas, Mol. Cryst. Liq. Cryst. **94**, 1 (1983).
[3] A. Lakhtakia and R. Messier, *Sculptured Thin Films: Nanoengineered Morphology and Optics* (SPIE Press, Bellingham, WA, USA, 2005).
[4] A. Lakhtakia, Mater. Sci. Eng. C **19**, 427 (2002).
[5] I. Abdulhalim, L. Benguigui, and R. Weil, J. Phys. Fr. **46**, 815 (1985).
[6] V. C. Venugopal and A. Lakhtakia, Proc. R. Soc. London A **456**, 125 (2000).
[7] J. B. Geddes III and A. Lakhtakia, Opt. Commun. **252**, 307 (2005).
[8] J. Adams, W. Haas, and J. Dailey, J. Appl. Phys. **42**, 4096 (1971).
[9] A. Lakhtakia and V. C. Venugopal, Microwave Opt. Technol. Lett. **17**, 135 (1998).
[10] A. Lakhtakia and I. J. Hodgkinson, Opt. Commun. **167**, 191 (1999).
[11] A. Lakhtakia and J. A. Polo Jr., J. Eur. Opt. Soc. Rapid Pub. **2**, 07021 (2007).
[12] K. Agarwal, J. A. Polo Jr., and A. Lakhtakia, J. Opt. A: Pure Appl. Opt. **11**, 074003 (2009).

[13] J. Gao, A. Lakhtakia, J. A. Polo Jr., and M. Lei, J. Opt. Soc. Am. A **26**, 1615 (2009); **26**, 2399 (2009) [corrections].
[14] M. I. D'yakonov, Sov. Phys. JETP **67**, 714 (1988).
[15] N. S. Averkiev and M. I. Dyakonov, Opt. Spectrosc. **68**, 653 (1990).
[16] D. B. Walker, E. N. Glytsis, and T. K. Gaylord, J. Opt. Soc. Am. A **15**, 248 (1998).
[17] A. N. Darinskii, Crystallogr. Rep. **46**, 842 (2001).
[18] J. A. Polo Jr., S. Nelatury, and A. Lakhtakia, Electromagnetics **26**, 629 (2006).
[19] J. A. Polo Jr., S. R. Nelatury, and A. Lakhtakia, J. Nanophoton. **1**, 013501 (2007).
[20] J. A. Polo Jr., S. R. Nelatury, and A. Lakhtakia, J. Opt. Soc. Am. A **24**, 2974 (2007).
[21] A. M. Furs and L. M. Barkovsky, Electromagnetics **28**, 146 (2008).
[22] S. R. Nelatury, J. A. Polo Jr., and A. Lakhtakia, Electromagnetics **28**, 162 (2008).
[23] I. Tamm, Z. Phys. A **76**, 849 (1932).
[24] H. Ohno, E. E. Mendez, J. A. Brum, J. M. Hong, F. Agulló-Rueda, L. L. Chang, and L. Esaki, Phys. Rev. Lett. **64**, 2555 (1990).
[25] J. Martorell, D. W. L. Sprung, and G. V. Morozov, J. Opt. A: Pure Appl. Opt. **8**, 630 (2006).
[26] A. Namdar, I. V. Shadrivov, and Y. S. Kivshar, Appl. Phys. Lett. **89**, 114104 (2006).
[27] A. M. Merzlikin, A. P. Vinogradov, A. V. Dorofeenko, M. Inoue, M. Levy, and A. B. Granovsky, Physica B **394**, 277 (2007).
[28] J. Gao, A. Lakhtakia, and M. K. Lei, J. Opt. Soc. Am. B **26**, B74 (2009).
[29] O. Takayama, L.-C. Crasovan, S. K. Johansen, D. Mihalache, D. Artigas, and L. Torner, Electromagnetics **28**, 126 (2008).
[30] S. R. Nelatury, J. A. Polo Jr., and A. Lakhtakia, Microwave Opt. Technol. Lett. **50**, 2360 (2008).
[31] O. Takayama, L. Crasovan, D. Artigas, and L. Torner, Phys. Rev. Lett. **102**, 043903 (2009).
[32] L. Torner, J. P. Torres, and D. Mihalache, IEEE Photonics Technol. Lett. **5**, 201 (1993).
[33] L. Torner, J. P. Torres, C. Ojeda, and D. Mihalache, J. Lightwave Technol. **13**, 2027 (1995).
[34] L.-C. Crasovan, D. Artigas, D. Mihalache, and L. Torner, Opt. Lett. **30**, 3075 (2005).
[35] H. C. Chen, *Theory of Electromagnetic Waves: A Coordinate-Free Approach* (McGraw-Hill, New York, NY, USA, 1983).
[36] T. G. Mackay and A. Lakhtakia, *Electromagnetic Anisotropy and Bianisotropy: A Field Guide* (World Scientific, Singapore, 2010).
[37] A. Lakhtakia and W. S. Weiglhofer, Proc. R. Soc. London A **453**, 93 (1997).
[38] M. Schubert and C. M. Herzinger, Phys. Status Solidi A **188**, 1563 (2001).
[39] J. A. Polo Jr., and A. Lakhtakia, Opt. Commun. **230**, 369 (2004).
[40] V. A. Yakubovich and V. M. Starzhinskii, *Linear Differential Equations with Periodic Coefficients* (Wiley, New York, USA, 1975).
[41] Y. Jaluria, *Computer Methods for Engineering* (Brunner-Routledge, New York, USA, 1996).